Jefferson fathered slave's last child

There is a long-standing historical controversy over the question of US President Thomas Jefferson's paternity of the children of Sally Hemings, one of his slaves[1–4]. To throw some scientific light on the dispute, we have compared Y-chromosomal DNA haplotypes from male-line descendants of Field Jefferson, a paternal uncle of Thomas Jefferson, with those of male-line descendants of Thomas Woodson, Sally Hemings' putative first son, and of Eston Hemings Jefferson, her last son. The molecular findings fail to support the belief that Thomas Jefferson was Thomas Woodson's father, but provide evidence that he was the biological father of Eston Hemings Jefferson.

In 1802, President Thomas Jefferson was accused of having fathered a child, Tom, by Sally Hemings[5]. Tom was said to have been born in 1790, soon after Jefferson and Sally Hemings returned from France where he had been minister. Present-day members of the African–American Woodson family believe that Thomas Jefferson was the father of Thomas Woodson, whose name comes from his later owner[6]. No known documents support this view.

Sally Hemings had at least four more children. Her last son, Eston (born in 1808), is said to have borne a striking resemblance to Thomas Jefferson, and entered white society in Madison, Wisconsin, as Eston Hemings Jefferson. Although Eston's descendants believe that Thomas Jefferson was Eston's father, most Jefferson scholars give more credence to the oral tradition of the descendants of Martha Jefferson Randolph, the president's daughter. They believe that Sally Hemings' later children, including Eston, were fathered by either Samuel or Peter Carr, sons of Jefferson's sister, which would explain their resemblance to the president.

Because most of the Y chromosome is passed unchanged from father to son, apart from occasional mutations, DNA analysis of the Y chromosome can reveal whether or not individuals are likely to be male-line relatives. We therefore analysed DNA from the Y chromosomes of: five male-line descendants of two sons of the president's paternal uncle, Field Jefferson; five male-line descendants of two sons of Thomas Woodson; one male-line descendant of Eston Hemings Jefferson; and three male-line descendants of three sons of John Carr, grandfather of Samuel and Peter Carr (Fig. 1a). No Y-chromosome data were available from male-line descendants of President Thomas Jefferson because he had no surviving sons.

Seven bi-allelic markers (refs 7–12), eleven microsatellites (ref. 13) and the minisatellite MSY1 (ref. 14) were analysed (Fig. 1b). Four of the five descendants of Field Jefferson shared the same haplotype at all loci, and the fifth differed by only a single unit at one microsatellite locus, probably a mutation. This haplotype is rare in the population, where the average frequency of a microsatellite haplotype is about 1.5 per cent. Indeed, it has never been observed outside the Jefferson family, and it has not been found in 670 European men (more than 1,200 worldwide) typed with the microsatellites or 308 European men (690 worldwide) typed with MSY1.

Four of the five male-line descendants of Thomas Woodson shared a haplotype (with one MSY1 variant) that was not similar to the Y chromosome of Field Jefferson but was characteristic of Europeans. The fifth Woodson descendant had an entirely different haplotype, most often seen in sub-Saharan Africans, which indicates illegitimacy in the line after individual W42. In contrast, the descendant of Eston Hemings Jefferson did have the Field Jefferson haplotype. The haplotypes of two of the descendants of John Carr were identical; the third differed by one step at one microsatellite locus and by one step in the MSY1 code. The Carr haplotypes differed markedly from those of the descendants of Field Jefferson.

The simplest and most probable explanations for our molecular findings are that Thomas Jefferson, rather than one of the Carr brothers, was the father of Eston Hemings Jefferson, and that Thomas Woodson was not Thomas Jefferson's son. The frequency of the Jefferson haplotype is less than 0.1 per cent, a result that is at least 100 times more likely if the president was the father of Eston Hemings Jefferson than if someone unrelated was the father.

We cannot completely rule out other explanations of our findings based on illegitimacy in various lines of descent. For example, a male-line descendant of Field

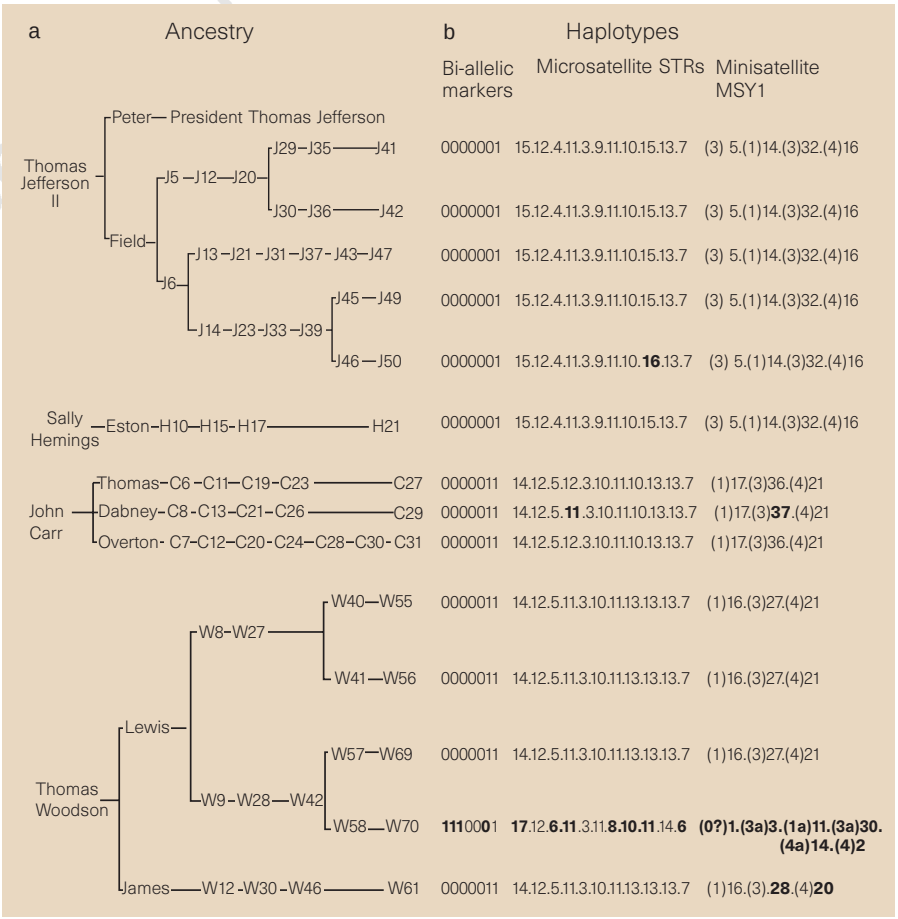

Figure 1 Male-line ancestry and haplotypes of participants. **a**, Ancestry. Numbers correspond to reference numbers and names in more detailed genealogical charts for each family. **b**, Haplotypes. Entries in bold highlight deviations from the usual patterns for the group of descendants. **Bi-allelic markers.** Order of loci: YAP-SRYm8299-sY81-LLY22g-Tat-92R7-SRYm1532. 0, ancestral state; 1, derived state. **Microsatellite short tandem repeats (STRs).** Order of loci: 19-388-389A-389B-389C-389D-390-391-392-393-dxys156y. The number of repeats at each locus is shown. **Minisatellite MSY1.** Each number in brackets represents the sequence type of the repeat unit; the number after it is the number of units with this sequence type. For example, J41 has 5 units of sequence type 3, 14 units of sequence type 1, 32 units of sequence type 3, and 16 units of sequence type 4.

Jefferson could possibly have illegitimately fathered an ancestor of the presumed male-line descendant of Eston. But in the absence of historical evidence to support such possibilities, we consider them to be unlikely.

Eugene A. Foster*, M. A. Jobling†, P. G. Taylor†, P. Donnelly‡, P. de Knijff§, Rene Mieremet§, T. Zerjal¶, C. Tyler-Smith¶

**6 Gildersleeve Wood, Charlottesville, Virginia 22903, USA*
e-mail: eafoster@aol.com
†Department of Genetics, University of Leicester, Adrian Building, University Road, Leicester LE1 7RH, UK
‡Department of Statistics, University of Oxford, South Parks Road, Oxford OX1 3TG, UK
§MGC Department of Human Genetics, Leiden University, PO Box 9503, 2300 RA Leiden, The Netherlands
¶Department of Biochemistry, University of Oxford, South Parks Road, Oxford OX1 3QU, UK

1. Peterson, M. D. *The Jefferson Image in the American Mind* 181–187 (Oxford Univ. Press, New York, 1960).
2. Malone, D. *Jefferson the President: First Term, 1801–1805* Appendix II, 494–498 (Little Brown, Boston, MA, 1970).
3. Brodie, F. M. *Thomas Jefferson: An Intimate History* (Norton, New York, 1974).
4. Ellis, J. J. *American Sphinx: The Character of Thomas Jefferson* (Knopf, New York, 1997).
5. Callender, J. T. *Richmond Recorder* 1 September 1802. [Cited in: Gordon-Reed, A. *Thomas Jefferson and Sally Hemings: An American Controversy* (Univ. Press of Virginia, Charlottesville, 1997)].
6. Woodson, M. S. *The Woodson Source Book* 2nd edn (Washington, 1984).
7. Hammer, M. F. *Mol. Biol. Evol.* **11,** 749–761 (1994).
8. Whitfield, L. S., Sulston, J. E. & Goodfellow, P. N. *Nature* **378,** 379–380 (1995).
9. Seielstad, M. T. *et al. Hum. Mol. Genet.* **3,** 2159–2161 (1994).
10. Zerjal, T. *et al. Am. J. Hum. Genet.* **60,** 1174–1183 (1997).
11. Mathias, N., Bayes, M. & Tyler-Smith, C. *Hum. Mol. Genet.* **3,** 115–123 (1994).
12. Kwok, C. *et al. J. Med. Genet.* **33,** 465–468 (1996).
13. Kayser, M. *et al. Int. J. Legal Med.* **110,** 125–133 (1997).
14. Jobling, M. A., Bouzekri, N. & Taylor, P. G. *Hum. Mol. Genet.* **7,** 643–653 (1998).

Coherent light scattering by blue feather barbs

The structural colours of avian feather barbs are created by the scattering of light from the spongy matrix of keratin and air in the medullary layer of the barbs[1–5]. However, the precise physical mechanism for the production of these colours is still controversial[1,3,4,6]. Here we use a two-dimensional (2D) Fourier analysis of the spatial variation in refractive index of the blue feather barbs of the plum-throated cotinga (*Cotinga maynana*, Cotingidae) to show that the colour is produced by constructive interference between light waves scattered coherently by the nanostructured keratin–air matrix of the barbs.

Mechanisms proposed to explain the production of structural colours of feather barbs fall into two classes, according to whether the vacuoles in medullary keratin scatter light coherently (with a relationship between the phases of waves scattered by different surfaces) or incoherently. In the Rayleigh and Mie scattering models[4,6], the colours are produced by incoherent scattering of smaller visible wavelengths by an array of spatially independent air vacuoles in the medullary keratin. Alternatively, in the constructive interference model, the colours are produced by interactions between light waves scattered coherently by the keratin–air matrix[1–3,5]. Out-of-phase waves will destructively interfere and cancel out, whereas in-phase waves will constructively reinforce one another and be reflected coherently. The phase relationships of scattered waves are determined by the size and spatial distribution of the scatterers[1,2,7]. Periodic spatial relationships between scatterers will produce consistent path-length differences among scattered waves and reinforce a limited set of wavelengths.

To investigate how the structural colour of feather barbs is produced, we apply an electromagnetic theory of coherent light scattering[7] that was developed to explain the transparency of the human cornea. In a quasi-random array of scatterers, coherent scattering is predicted only for light waves with a wavelength of twice that of the largest components of the Fourier transform of the spatial variation in refractive index[7]. We performed a discrete 2D Fourier analysis of digitized transmission electron micrographs of cross-sections of the medullary keratin from the blue feather barbs of *C. maynana* to examine whether it has periodic spatial variation in refractive index. The spongy medullary layer of *C. maynana* barbs consists of a matrix of keratin bars with air vacuoles of strikingly uniform diameter and spacing[2]. The matrix has no planes of symmetry and is randomly orientated to the surface of the feather. The 2D Fourier power spectrum of the medullary keratin matrix shows a nearly circular ring around the origin 0.0059 nm^{-1} in diameter (Fig. 1a). This ring indicates that the tissue has a highly ordered, nanoscale spatial variation in refractive index that is nearly uniform in all directions.

Reflection spectra of the blue feather barbs display a peak between 500 and 520 nanometres (Fig. 1b). We used the 2D Fourier power spectrum to predict the reflectance spectrum of these barbs. The

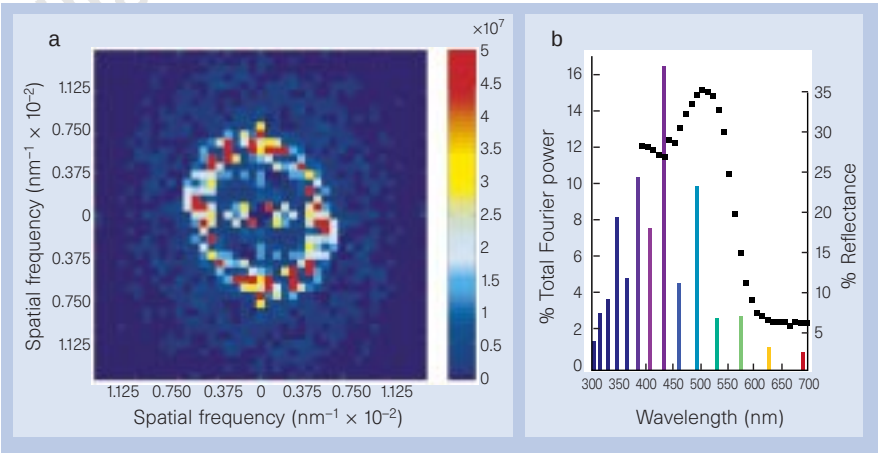

Figure 1 Two-dimensional Fourier power spectrum and observed and predicted reflectance spectra of a blue feather barb of *Cotinga maynana*. a, 2D Fourier power spectrum of the spongy medullary keratin matrix of a blue feather barb. b, Observed reflectance spectrum of a blue feather barb (black squares, right axis) and predicted reflectance spectrum (bars, left axis) based on the 2D Fourier power spectrum (a). The discrete Fourier transform describes how a signal or image is composed of different periodic component waves[10]. A 2D Fourier analysis was conducted using the 2D Fast Fourier Transform algorithm in MATLAB[11] on a digitized 500-$pixel^2$ image of a transmission electron micrograph (magnification, × 29,000)[2]. The image was processed in MATLAB using variance rescaling with block processing and median filtering[11]. The 2D Fourier power spectrum (a) resolves the spatial variation in optical density in the tissue into its periodic components in any direction in the plane from all points. The size and direction of any component spatial frequency is given by the length and direction of a vector from the origin to that point. The squared amplitude of the component is given by the colour (scale bar on the right). The ring indicates a highly ordered, nanoscale fluctuation in optical density moving in any direction in the plane of the tissue at a spatial frequency of about 0.0059 nm^{-1}. Reflectance of blue feather barbs (b, squares, right axis) was measured using a Zeiss microspectrophotometer at 30 wavelengths between 400 and 700 nm[12]. The predicted reflectance spectrum (b, bars, left axis) expresses the percentage of the total power distributed among the components of the 2D Fourier power spectrum over all directions. The predicted reflection spectrum was calculated using the radial average of one quadrant of the 2D Fourier power spectrum with half-pixel width intervals, normalizing the volume under the rotated radial average function to one, calculating the volume under radial sections of the radial average Fourier power function, multiplying these volumes by twice the mean refractive index (1.283), estimated from the micrographs using the refractive indices of keratin (1.54) and air (1.00)[2], and plotting these values as wavelengths in nanometres.